Int. J. Electrochem. Sci., 16 **(2021)** Article Number: 211036, doi: 10.20964/2021.10.37

International Journal of
ELECTROCHEMICAL
SCIENCE
www.electrochemsci.org

Fabrication and Application of Bismuth-Film Modified Glassy Carbon Electrode as sensor for Highly Sensitive Determination of Cetirizine Dihydrochloride in Pharmaceutical Products and Water Samples

Eman A. Al-Harbi

Department of Chemistry, Faculty of Science, Taibah University, Al-Madinah Al-Minawara 42353, Kingdom of Saudi Arabia
E-mail: eahharbi@taibahu.edu.sa

Received: 20 June 2021 / *Accepted:* 9 August 2021 / *Published:* 10 September 2021

The considerable necessity to detect and analyze cetirizine dihydrochloride (CTZ) residues has motivated the development of cost-effective and high-performance sensing probes. A highly sensitive, square wave anodic stripping voltametric (SW-ASV) methodology has been employed in correspondence with a bismuth-film platted glassy carbon electrode (BiF/GCE) for the establishment of the CTZ drug at trace levels in an aqueous media of pH 8.0. The nature and mechanism of the electrode reactions have been ascribed at BiF/GCE for the square wave and cyclic voltammetry techniques. Under the optimized parameters and at pH 8.0, a well-defined square wave (SW) anodic stripping peak at + 0.48 V versus Ag/AgCl was detected. The plot of the anodic current versus known concentrations of CTZ was linear in the range of [$5.0 \times 10^{-9} - 1.2 \times 10^{-6}$ mol L^{-1}] (R2=0.999) with limits of detection (LOD) and calculation (LOQ) of 1.5×10^{-9} and 5.0×10^{-9} mol L^{-1}, respectively. The acquired SW-ASV technique was successfully employed for the determination of nano concentrations of CTZ in pharmaceutical preparations and water samples on BiF/GCE. These method provides a good correlation with the data obtained for the deduction of CTZ in numerous matrices through the spectrophotometric approach.

Keywords: Stripping voltammetry; Cetirizine dihydrochloride; Bi film modified electrode; Glassy carbon electrode; Pharmaceutical preparations; Environmental water.

1. INTRODUCTION

Cetirizine dihydrochloride (CTZ) is a synthetic piperazine derivative and viable antihistamine, utilized in the therapy of periodic and permanent allergic rhinitis, hay fever, chronic urticaria or pruritus of the allergic origin, Fig.1, [1-3]. The physicochemical properties of CTZ encompass the prevention of

histamine permeability through blood–brain barriers and the hindering of histamine activity through its selective inhibition of the binding affinity between the H1-histamine and their respective receptors on the surface of cells, all without instigating adverse impacts, including: sedation, drowsiness, and diminished cognitive processing [1, 4-6]. CTZ is constructed from a racemic combination of the levocetirizine (R-cetirizine) and dextrocetirizine (S-cetirizine) enantiomers, which enables an assortment of biological and pharmacological behaviors [7]. The diversity in enantiomer molecular structure and ratio manipulates these behaviors, such as CTZ's affinity with H1-receptors, through the augmented performance of one of the enantiomers, namely levocetirizine [8].

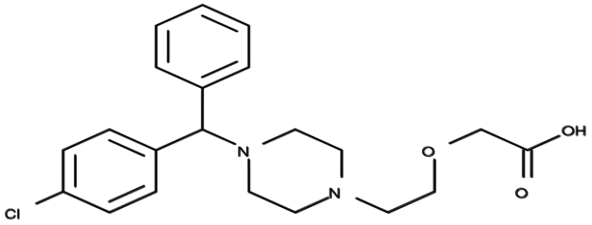

Figure 1. Chemical structures of cetirizine.

An extensive series of the analytical procedures has been documented for the trace detection of the entitled drug in its pure form for pharmaceutical preparation and employment, including: spectrofluorimetry [9], spectrophotometry [10-13], flow injection-chemiluminescence (FI-CL)[14], titrimetry and conductimetry [15], calorimetry [16], potentiometry [17], gas chromatography [18], liquid chromatography [19, 20], HPLC methods[21-24], and reversed-phase HPLC (RP-HPLC) [25-27]. A majority of these procedures necessitate sample pretreatments (extraction, derivatization, complex formation, etc.), which exhaust monetary and time expenditures through the purchase of organic solvents and sophisticated instrumentation. The determination of the CTZ was also achieved by electrochemical techniques, such as square wave voltammetry (SWV) and cyclic voltammetry (CV) [28-30]. Among these approaches, the utilization of BiF/GCE has not been tested so far for the trace determination of the CTZ molecule. Thus, the current work is centered on: I) investigating the redox activity of the cetirizine drug at the BiF/GCE; II) assigning the electrode type mechanism of the observed electrode couples at BiF/GCE; III) developing a low cost square–wave-anodic stripping voltammetry (SW-ASV) founded on the BiF/GCE, and finally IV) testing the utility of the established probe for the determination of the trace levels of CTZ residues in pharmaceutical preparations of water samples (tap-and wastewater).

2. EXPERIMENTAL PROCEDURES

2.1. Chemicals and reagents

All the chemicals were of analytical grade and used without further purifications (BDH, Poole, England). Low density polyethylene bottles (LDPE), pre-cleaned with detergent such as HNO_3 (2.0 mol L^{-1}) and 50% HCl (Analar), were used for real samples storage and collection. Cetirizine hydrochloride was obtained from Aldrich Chemical Co. (Milwaukee, Wisconsin, USA) and utilized for preparing more

diluted working solutions (0.1×10^{-8} – 0.1×10^{-5} mol L^{-1}) using deionized water (Millipore, Milford, MA USA). A series of (0.04 M) Britton–Robinson buffers (B-R) (pH 2.0 - 11.0) was formulated as previously documented [31]. Pharmaceutical formulations containing CTZ were obtained from the local pharmacy at Jeddah, Saudi Arabia.

2.2. Instruments

A Metrohm 746 VA trace analyzer along with 747 VA stand borosilicate (Metrohm) voltammetric cell were used at 25±1°C for recording the electrochemical experiments. A glassy carbon electrode (GCE) (1 mm diameter, BAS, USA) or BiF/GCE was used as a working electrode with a Ag/AgCl/KCl (3 mol L^{-1}) and a Pt wire (BAS model MW-1032) as reference and auxiliary electrodes, respectively. Deionized water was provided *via* Milli-Q Plus system (Millipore, Bedford, MA, USA). A digital-pH-meter (MP 220, Metter Toledo) and digital-micro -pipettes (Volca) were used for pH measurements and preparation of more diluted solutions. A Scanning Electron Microscope (SEM) model JEOL USA Inc., JSM6301-F (Peabody, MA, USA.) with an accelerating voltage (10 kV) in low vacuum SEM mode, at 20 mm working distance was used.

2.3 Preparation of (BiF/GCE)

The surface of the GCE was first refined thoroughly with slurries prepared from 0.03 and 0.05μm alumina (Al_2O_3) powder, on a soft cloth, sequentially and then sonicated in 1:1 HNO_3, ethanol and H_2O for 5 min to remove alumina particles and other contaminants and finally dried in Nitrogen atmosphere. In the voltammetric cell, the GCE was submerged into an aqueous solution encompassing 0.1 M acetate buffer solution (10 mL) and $Bi(NO_3)_3$ (900 μL, 1.0 gL^{-1}) at pH 4.5–5.0. The Bi film was electrochemically deposited on the GCE *via* cyclic voltammogram (CV) of the test solution at a potential range of -0.5 - 1.7 V for 25 cycles and 100 mVs^{-1} under stirring [32-34].

2.4. Recommended SW-ASV procedures

Accurate volume (10.0- 100.0 μL) of cetirizine HCl (0.1×10^{-8} – 0.1×10^{-5} mol L^{-1}) was added to the Britton-Robinson buffer (B-R) (pH =8) which pipetted into a volumetric cell. The solution was de-aerated and stirred followed by recording voltammogram for supporting electrolyte and cetirizine under constant operational electrochemical parameters as follows; range of potential window [-0.7 to 0.7 V], accumulation time of 240 s; - 0.1 V accumulation potential; starting potential 0.3 V; 50 Hz frequency; pulse amplitude 80 mV and 80 mVs^{-1} scan rate. The SW-ASVs measurements were recorded at the BiF/GCE *vs.* Ag/AgCl. The concentration of cetirizine was computed from calibration plot after the blank correction.

2.5. Method validation

The established technique was authenticated through the linear dynamic range, relative standard deviation (RSD), LOD, LOQ, repeatability, accuracy, robustness and selectivity. Repeatability was assessed through (intra-day) measurements (n=5) at five different concentrations of cetirizine. The intermediate (inter-day) precision was assessed for 5 consecutive days. The recovery assays for five different concentrations of CTZ were used to evaluate the accuracy of the planned method.

2.6. Analytical utility

2.6.1. Detection of CTZ in pure form and pharmaceutical formulations reparations

Twenty tablets of Zyrtec® and Zertazine® (10 mg CTZ /tablet) were crushed in a small glass mortar until a powdered form was attained. An accurate mass of powder (average mass /tablet) was dissolved in the ethanol (5 mL), sonicated for 20 min. The sample's solution was shaken in a mechanical shaker for 25 min at room temperature to obtain a complete dissolution of the active material and then left for two hours then filtered (0.45 mm Milli-pore filter Gelman, Germany). The filtrate and the washing solutions were precisely relocated to the measuring flask (25 mL) and completed to the mark with ethanol. A volume (10.0 µL) of the test solution was placed into the voltammetric cell in the presence of B-R buffer (10 mL, pH = 8) as a supporting electrolyte. Under the optimized parameters, the SW-ASVs of the test solution were recorded before and after the addition of known CTZ concentration. The current signal at E_{pa} = +0.43 V was measured before and after each addition of the standard CTZ, and finally the unknown CTZ concentration was calculated from the linear plot of the standard addition.

2.6.2. Determination of cetirizine in tap and industrial water samples

Tap and industrial wastewater samples were gathered from the laboratories of the Chemistry Department, Taibah University, Al-MadinahAl-Minawara and the municipal discharge station in Jeddah city, KSA, respectively. After the samples were filtered using Whatman filter papers, the filtration of tap-water (1 mL), adjusted by 9 mL of B-R buffer (pH=8), was placed into the cell. The $i_{p,a}$ was measured by the recommended SW-ASV procedure. Same protocol has been employed to tap-water samples after the addition of different volumes (10-40 µg mL^{-1}) of standard CTZ solutions. Regarding the filtration of the industrial wastewater, an accurate volume of the standard cetirizine solutions (0.5-2 mL, 0.3 µg mL^{-1} in ethanol) was spiked to the water samples (0.5-1.0 L) to get a final concentration of [0.075–0.3 µg mL^{-1}]. The solutions were passed through C-18 cartridge (precedingly pre-conditioned with 2.0 mL of methanol followed by one mL of H_2O) at 5.0 mL min^{-}flow rate [35, 36]. The cartridge was bathed several times (5.0×1 mL) with water. The CTZ drug was recovered quantitatively after elution with ethanol (2×5 mL) at 0.5 mL min^{-1} flow rate. The ethanol fractions were collected, combined together and measured by the recommended methodology.

3. RESULTS AND DISCUSSION

3.1. Characterizations of the BiF/GCE by SEM

The surface morphology images of the of GCE and its bismuth (Bi/GCE) modified counterpart were characterized by scanning electron microscopy (SEM), Fig 2. As observed from the obtained Figure, the bismuth deposition appears as dendritic areas on the GCE surface. The film offers considerable surface area for the electrode which enhances the electrochemical adsorption and detection of CTZ.

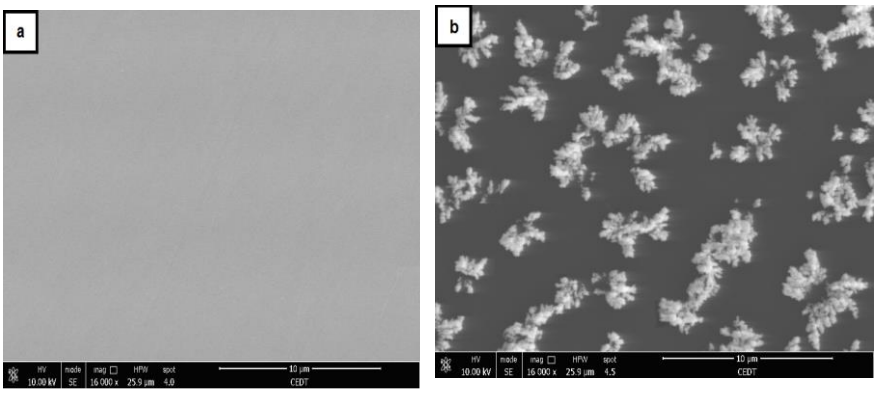

Figure 2. SEM of bare GCE (a) and bismuth-film deposited on GCE (b) at accelerating voltage; 10 kV, magnification; 16,000X and scale size 10 μm.

3.2. Redox characteristics of CTZ drug

The SW-ASV behavior was investigated under diverse experimental conditions, such as varying the: accumulation time, deposition potential, and pH, in order to enhance the stripping current intensity. The sensitivity of the analyte detection on the BiF/GCE was dependent on the fluctuating conditions of the declared parameters [37]. The pH of the medium is the most imperative parameter that controls the electrolysis course by manipulating the shape of the voltammogram's peak current and potential, which was centered on in this work and explored through the employment of the B-R buffer with a pH of [2.0-11.0] corresponding to the utilized concentration of CTZ (1×10^{-8} mol L^{-1}) at BiF/GCE (Fig. 3). The plot of the anodic peak current and potential versus the pH for the trace CTZ residues was illustrated in (**Figure S1**), where the optimum current response was detected at pH 8.0 and a sharp, distinct anodic peak was identified at +0.43 V. The stripping peak appeared at the more positive potential than the re-oxidation of Bi (proving the efficient usability of BiFE for the detection of CTZ), which is consistent with the formerly documented research work in the case of copper[38] and silver[39], also mercury at the CuFE [40] and mercury (II) in the SbF electrode[41, 42]. The figure depicting this plot demonstrated linearity with a slope of 51 mV/pH according to the following equation:

$$E_{p,\,a} = 0.051\ pH + 0.087,\ (R^2 = 0.959) \qquad \textbf{(1)}$$

Additionally, in order to heighten the current intensity further, the solution's pH was elevated, which shifted the oxidation peak potential ($E_{p,a}$) to more positive values and approximated the slope value to the Nernst quantity, confirming the involvement of a proton/electron transfer [33]. The increased activity of the surface area, coupled with the promising electrochemical behavior from the BiF/GCE, may have also accounted for the discerned response. At pH > 8.0, the observed behavior of the anodic peak current (ip,a) revealed a decline in the drug's concentration detection, which is probable due to the decrease of CTZ within the medium. This concentration decrease is instigated through the diminution of the BiF/GCE electrode's sensitivity, due to the the reduction rate of H^+ to H_2 on the sensing surface, which arises as a result of pH quantities > 8.0 and is the motivating reason behind the selection of pH = 8.0 for further studies.

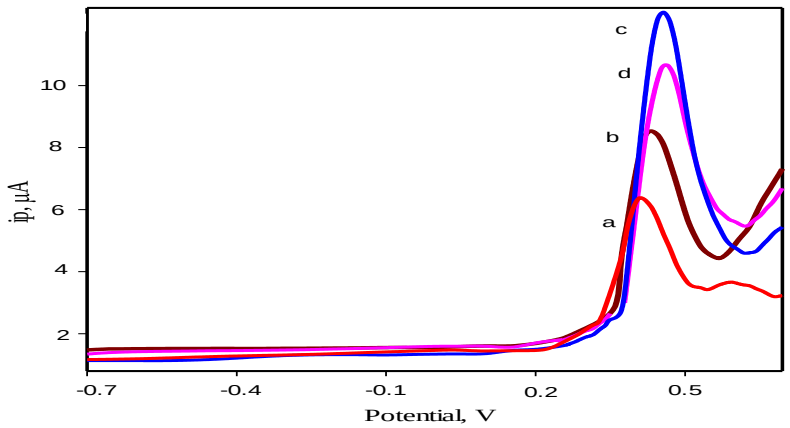

Figure 3. SW-CSVs of CTZ (1×10^{-8} mol L^{-1}) at pH 6 (a); pH 7 (b); pH 8 (c); pH 9-10(d) at BiF/GCE.

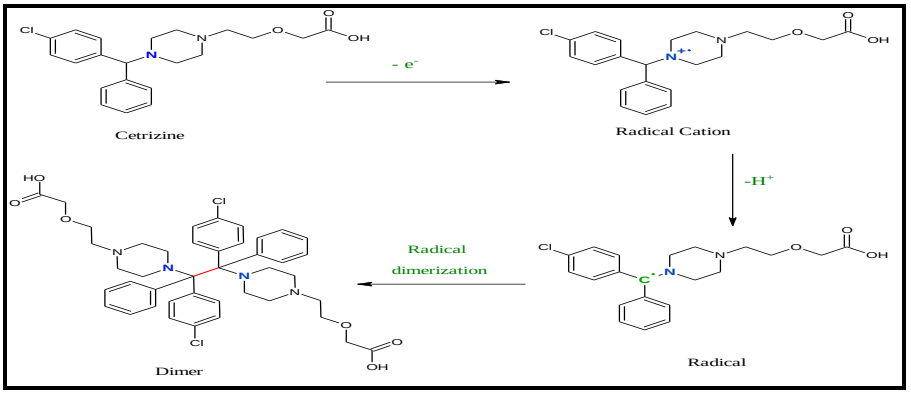

Scheme 1. The proposed scheme for the electrochemical oxidation of CTZ.

The redox characteristics of the CTZ drug at BiF/GCE were investigated through cyclic voltammetry (CV) at pH 8.0. Figure 4 illustrates representative CVs at different scan rates (ν = 20.0-1400 mVs^{-1}) in a B-R buffer. The attained voltammograms revealed a well-defined anodic peak in all scan rates. Upon elevating the scan rate to 100 mV/s, the potential of the CTZ's anodic peak (Ep,a) anodically shifted towards a more positive potential, verifying the irreversible quality of the electrode

procedure [29]. On the reverse scan, no cathodic peaks were detected in any of the scan rates, which similarly substantiate the irreversibility of the electrode process hypothesis. Furthermore, the impact of the sweep rates (20.0-1400 mV/s) on the cyclic voltammograms at pH 8.0 was analyzed. A proposed electrochemical oxidation mechanism of CTZ, involving the transfer of one proton/electron (H=/e), is illustrated in Scheme 1 [43].

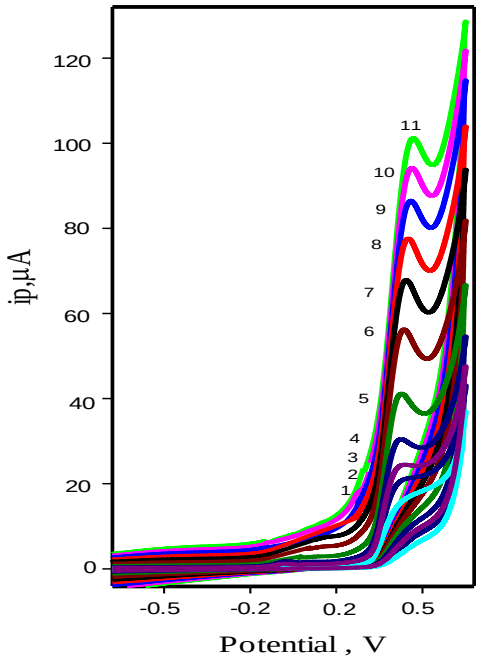

Figure 4. Cyclic voltammograms of CTZ drug at pH 8.0 at various scan rates 20 (1), 60 (2), 80 (3), 100 (4), 200 (5), 400 (6), 600 (7),800 (8), 1000 (9), 1200 (10), and 1400(11) mVs^{-1} at BiF/GCE vs. Ag/AgCl electrode.

The plot of the $i_{p,a,}$ µA *versus* the square root of the sweep rate ($\nu^{1/2}$) was discovered to be linear (**Figure S2**) with a slope of 0.58, approximate to the theoretical quantity [44]. Thus, it can be concluded that the electrode process is a combination of the diffusion- and adsorption-controlled reactions [44, 45]. The linear plot of log $i_{p,a}$ *versus* log ν (20.0-1400 mVs^{-1}) (**Figure S3**) verified the irreversible nature of the electrode procedure [35, 36]. The slope of the lot was 0.85 (R^2=0.9998), which is greater than 0.5, revealing that the electrode process is an adsorption-controlled approach and further substantiates the irreversibility of the electrochemical processes observed [44, 46].

The cyclic voltammogram's linear plot of the $E_{p,a}$ of CTZ *versus* log ν in the range of ν = 20.0-1400 mVs^{-1} at pH 8.0 utilizing BiF/GCE (R^2= 0.999) confirmed an irreversible factor of the electrode process (**Figure S4**). Based on the Laviron's equation [47], the computed values of α and αn as calculated from the slope of the linear plot (Fig. S4) were found to be 0.58 and 2.0, respectively. The value of α (0.58) is higher than 0.5, similarly supporting the electrode reaction's irreversibility [44, 47]. The plot of the current function ($i_{p,a\,/}\,\nu^{1/2}$) versus the sweep rate decreased continuously, indicating that the redox process proceeded according to the renowned coupled homogeneous reaction of the EC type mechanism

[44]. In this class of mechanism, the value of $i_{p,a} / \nu^{1/2}$ decreased continuously with the upsurge of the scan rate for an irreversible electrochemical process, [46, 47]. Thus, the irreversible redox step for the formed products preceded in a swift, supplementary chemical reaction [47]. The electrode surface area (A) is calculated *via* the Randles–Sevick equation[48]:

$$I_{p,a} = 2.69 \times 10^5 \, A C_0 \, n^{3/2} \, D_R^{1/2} \, \upsilon^{1/2} \qquad \textbf{(2)}$$

where, A is the electrochemically–active area of the electrode surface (cm^2), C_0 is the concentration of CTZ HCl, n is the number of electrons, D_R is the diffusion coefficient, and ν is the sweep rate. For n = 1, the value of A for the bare GCE was 0.067 Cm^2 and for the BiF/GCE was 0.14 Cm^2. As anticipated, the results divulged that the modified BiF/GCE increased the bare GCE's electrochemically-active surface area due to its high specific surface area and excellent conductivity film. Additionally, the electro active species (surface coverage, Γ) was quantified from the CVs by the following equation [46, 49]:

$$I_{p,a} = n^2F^2A\Gamma\upsilon / 4RT \qquad \textbf{(3)}$$

where, n is the number of electrons, A is the electrochemically-active area of the electrode (cm^2), R is the gas constant, and T is the absolute temperature (Kelvin). For n = 1, the value of Γ is 1.40×10^{-6} mol cm^{-2}, demonstrating the successful appliance of the SW-ASV technique for the determination of CTZ, utilizing BiF/GCE, conforming with the appearance of the multilayer surface species.

3.3. Analytical parameters

The preliminary study on the redox characteristics of the CTZ drugs at Bi/GCE using CVs and SW-ASVs results revealed a maximum peak current and sensitivity with a distinctive anodic peak potential at + 0.48 V *versus* Ag/AgCl at pH 8.0 (Figs. 2 & 3).

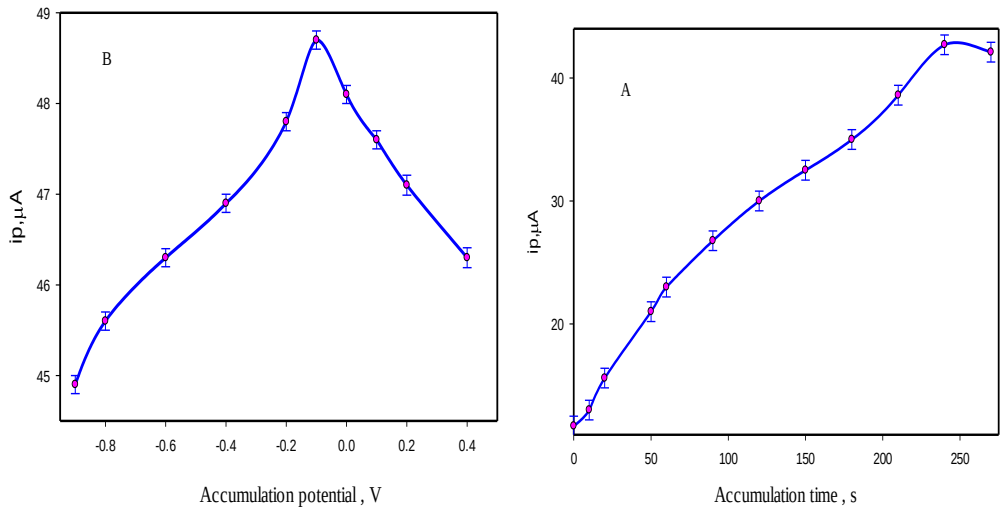

Figure 5. Plot of the anodic peak current ($_{ip,a}$) of CTZ drug at BiF/GCE (pH 8.0) vs. :(A) accumulation time (t_{acc}) E_{acc} =-0.9 V, (B) deposition potential.

Hence, a complete investigation on the impact of several analytical parameters on the current signal of the oxidation peak, using the SW-ASVs of the drug at BiF/GCE, was critically addressed.

The influence of the accumulation time (0.0 to 270 s) on the sensitivity of the stripping peak at + 0.48 V *versus* Ag/AgCl and at accumulation potential value = -0.75V was examined. The results are shown in Fig. 5(A), where, a distinctively sharp stripping peak and maximum peak current ($i_{p,a}$) was achieved at 240 s and leveled off at higher deposition time due to the adsorption saturation of the CTZ at the BiF/GCE surface. Thus, a deposition time of 240 s was adopted in the subsequent study. Meanwhile, the impact of the deposition potential (-0.75 – +0.4 V) on the anodic peak current at BiF/GCE *versus* Ag/AgCl was appraised (results are illustrated in Fig.5(B)). A maximum anodic peak current was attained at an accumulation potential of -0.1V and decreased markedly at lower potentials. Thus, in the subsequent study, an accumulation potential of -0.1V was chosen. The influence of the sweep rate (20–100 mV s^{-1}) at BiF/GCE on the $i_{p,a}$ of the CTZ drug was investigated using SW-ASV at pH 8.0. The results illustrated that the elevation of the sweep rate results in a subsequent elevation of the anodic current $i_{p,a}$ value (**Figure S5**). According to the acquired results, the optimized peak resolution, best background, sensitivity and width of the anodic peak was noticed at 80 mV s^{-1} scan rate, which was chosen for further investigation.

Pulse amplitude represents an important parameter in the SW-ASVs, thus the impact of the pulse amplitude in the range of 20 to 100 mV to determine the CTZ drug was appraised. The anodic current increased up to 80 mV pulse amplitude then leveled off with higher values (**Figure** 6). A pulse amplitude > 80 mV caused broadening of the anodic voltammogram where the anodic peak shifted anodically and its widths further increased with the increase in the pulse's height. Therefore, a pulse amplitude of 80 mV was selected as an optimized value for further examination. The influence of the frequency (10 to 90 Hz) on the SW-ASV signals was appraised. A maximum anodic current was noticed at 50 Hz frequency. Thus, a frequency of 50 Hz was assumed in the following work. Meanwhile, the impact of fluctuating the starting potential at BiF/GCE vs. Ag/AgCl from -0.1 to 0.45 V on the $i_{p,a}$ was also recorded. A maximum peak current with distinct anodic peak was noticed at +0.3 V starting potential. Further increase in the starting potential revealed a gradual decline in the current value, attributable to the previous reduction of the drug. Thus, a value of +0.3 V was preferred as a starting potential in the subsequent study.

3.4. Analytical performance and figures of merits

Under the optimized parameters of pH 8.0, accumulation time of 240 s, deposition potential of -0.1V, frequency of 50 Hz, scan rate of 80 mV s^{-1}, 0.3 V starting potential, and 80 mV pulse amplitude, the SW-ASVs of CTZ drug were recorded. As anticipated, the $i_{p,a}$ at 0.48 V increased linearly with increasing the drug concentrations from 5.0 $\times 10^{-9}$ to 1.2$\times 10^{-6}$ mol L^{-1} (R^2=0.999) as shown in Fig. 6 and the following regression equation:

$$i_{p,a}\ (\mu A) = 1.51\times 10^{8}\ C\ (\text{mol } L^{-1}) + 2.67 \quad , R^2 = 0.999 \qquad (4)$$

where, $i_{p,a}$ is anodic peak current stripping voltammetric in amperes, C is the CTZ concentration (mol L^{-1}) and R^2 is the correlation coefficient. At concentration > 1.2×10^{-6} mol L^{-1}, the linear plot stabilized due to the adsorption saturation [50]. The values of the LOD ($LOD=3S_{y/x}/b$) and LOQ ($LOQ= 10S_{y/x}/b$) [51], where $S_{y/x}$ is the standard deviation of y-residual and b is the slope of the calibration plot of CTZ, were revealed to be 1.5×1^{-9} mol L^{-1} and 5.0×10^{-9} mol L^{-1}, respectively. The obtained values are the average quantity of at least five trials performed for each measurement. The calibration sensitivity of the developed technique was evaluated as 1.51×10^{8} µA M^{-1}.

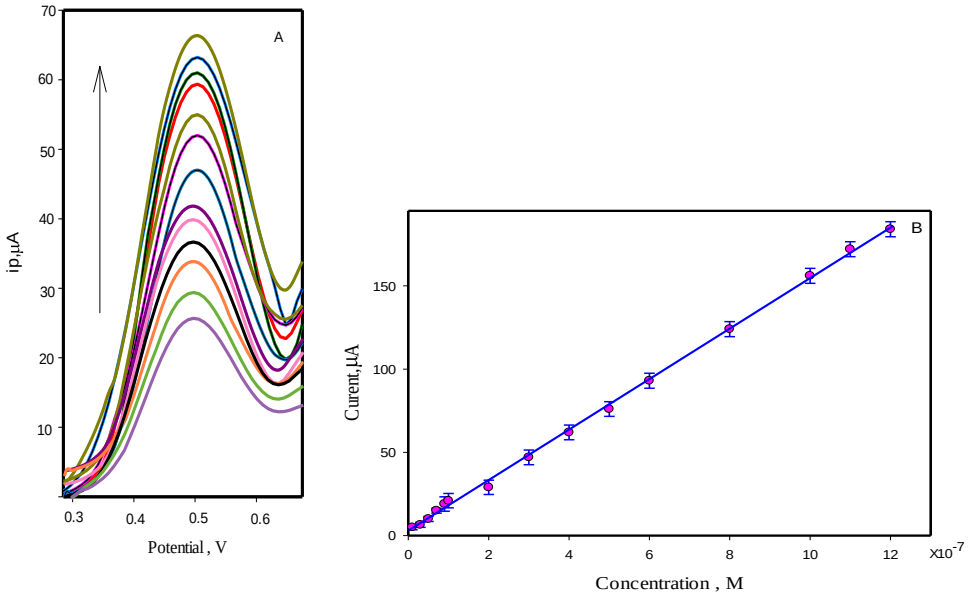

Figure 6. SW- ASV voltammograms (A) and calibration curve (B) of CTZ drug at BiF/GCE (pH 8.0), at different concentrations of CTZ (0.5×10^{-8}–1.2×10^{-7} mol L^{-1}).

The repeatability of the $i_{p,a}$ was estimated by consecutive intra-day measurements (n=5) of CTZ (1×10^{-8} mol L^{-1}) with a relative standard deviation (RSD= ± 2.81%). Thus, the repeatability for inter-day precision was estimated for four days with (RSD = ± 3.7%). The main analytical qualities of the developed SW-ASV method (LDR, LOD and LOQ) were compared favorably with many spectrophotometric, chromatographic and electrochemical methods [19, 21, 23, 25, 26, 28, 52, 53] as summarized in Table 1. The developed electrode has a large linear response range compared to reported electrochemical techniques and possess the lowest LOD for CTZ detection. Also, the sensitivity of the developed sensor, utilized in the detection of CTZ, is higher in comparison with other electrodes proposed in previous studies[28-30].

Table 1. Analytical features of number of other described techniques for the detection of CTZ drug*

Method (Electrode)	LOD (M)	LOQ (M)	LDR (M)	Regression equation, Correlation coefficients, R^2	Reference
$^1D_{239}$	0.135×10^{-6}	0.36×10^{-6}	1.20×10^{-6} - 10.0×10^{-6}	$Y=1.65\times10^{-2}$ C(μgml^{-1})- 4.7×10^{-4}; R^2 =0.9998	[52]
CE	5.45×10^{-6}	1.60×10^{-5}	2.30×10^{-5}- 1.15×10^{-4}	$Y = 1.55 \times 10^4$ C (M) + 0.0125; R^2 =0.9998	[23]
CZE	0.6×10^{-6}	2×10^{-6}	2×10^{-6}- 50×10^{-6}	Y = 0.0072 C(μgml^{-1}) -0.0089; R^2 =0.9982	[53]
RP-LC	0.5×10^{-9}	-	10×10^{-9} - 500×10^{-9}	Y=0.0027 C(ngml^{-1})-0.0054; R^2=0.998	[19]
HPLC	0.10×10^{-6}	0.34×10^{-6}	1.2×10^{-6}- 3.8×10^{-6}	Y=4.20 C (μgml^{-1})- 0.15; R^2 =0.9994	[21]
RP-HPLC	3.70×10^{-8}	12.33×10^{-8}	0.5×10^{-6}- 50×10^{-6}	$Y = 1.74\times10^4$C (μgml^{-1}) + 3.65×10^3; R^2 = 0.9999	[25]
RP-HPLC	0.10×10^{-6}	0.30×10^{-6}	1.25×10^{-6} - 10×10^{-6}	Y= 0.1498C (μgml^{-1})- 0.0390; R^2 =0.9998	[26]
SWV (Ru-TiO_2/MWCNTs-CPE)	3.1×10^{-9}	10.4×10^{-9}	3.0×10^{-8} -1.0×10^{-6}	Y= 34.26 C (M)+ 7.436 ; R^2 =0.919	[28]
CV (MWCNT modified GCE)	7.07×10^{-8}	-	5.0×10^{-7} - 1.0×10^{-5}	Y = 13.32C (μM) + 66.64; R^2 = 0.994	[29]
SW (p.GPE)	1.6×10^{-7}	-	0.50×10^{-6} - 10.0×10^{-6}	Y = 0.477C (μM) + 0.141 R^2 =0.998	[30]
SW-ASV (BiF/GCE)	1.5×10^{-9}	5.0×10^{-9}	5.0×10^{-9} - 1.2×10^{-6}	$Y = 1.51\times10^8$ C (M) + 2.67; R^2 =0.999	Present work

*LDR = Linear dynamic range ; 1D239 = First Derivative Spectrophotometry; CE = Capillary Electrophoresis; CZE = Capillary Zone Electrophoresis ; RP-LC = Reversed Phase Liquid Chromatography ; HPLC = High-Performance Liquid Chromatography; RP-HPLC = Reversed-Phase High-Performance Liquid Chromatography; Ru TiO2/MWCNTs-CPE =Carbon Sensor Fabricated with Coalesced Ruthenium-Doped Titanium Dioxide; CV= Cyclic voltammetry; MWCNT modified GCE= Glassy carbon electrode modified with multiwalled carbon nanotubes; p.GPE= pretreated graphite pencil electrode.

3.5. Selectivity and interference study

The recommended SW-ASV method was used for the determination of CTZ (1.0×10^{-8} mol L^{-1}) in the incidence of diluents, excipients, and active ingredients, such as: magnesium stearate, sodium

lauryl sulfate, talcum powder, glucose, sucrose, lactose, fructose, starch, and mannitol powder, which have been employed in pharmacological preparations. Each excipient (0.01–0.1 g) was spiked to a desired CTZ concentration (1.0×10^{-8} mol L^{-1}). The acceptable limit was characterized as the excipient level, instigating a relative standard deviation of ±3.0% at the magnitude of $i_{p,a}$ at +0.43 V for the CTZ drug. The recovery data indicated that no suggestive alterations on the $i_{p,a}$ by more than ±3% have been observed. Moreover, the tested excipients and interfaces have negligible effects on the proposed SW-ASV procedure. The developed methodology is considered a selective procedure towards the tested analyte.

3.6. Analytical applications

3.6.1. Detection of CTZ HCl in pharmaceutical products

The propositioned technique was employed by performing a CTZ analysis in both pure forms and pharmaceutical formulations e.g., Zyrtec and Zertazine tablets (10 mg/tablet) containing cetirizine *via* the standard addition method. The recovery percentage (97.3-98.5) for the CTZ analysis is given in Table 2, where the obtained data were discovered to be in accordance with the previous products attained from the official spectrophotometric procedure [16].

Table 2. Determination of cetirizine dihydrochloride in some pharmaceutical formulations.

Pharmaceutical preparations	**Function**	**SW-ASV**	**UV-Vis [16]**
Zertazine®, (Riyadh Pharm., Saudi Arabia) (10 mg/ tablet)	Average*	10.1±0.09	**9.8±0.08**
	Recovery	101	**98.0**
	RSD	0.89%	**0.81%**
	t-value**	**1.50 (1.86)**	
	F-value**	**2.60 (6.39)**	
Zyrtec®, (Glaxosmithkline, Italy) (10 mg/ tablet)	Average	9.9±0.1	**9.8±0.07**
	Recovery	99.0	**98.0**
	RSD	1.01%	**0.71%**
	t-value	**1.29 (1.86)**	
	F-value	**2.14 (6.39)**	

* Average recovery of five measurements ± SD; **The corresponding theoretical values for F and t are figures in parenthesis at P = 0.05.

3.6.2. Analysis of cetirizine in tap- and wastewater

The determination of the CTZ residues in tap and industrial wastewater samples by the recommended SW-ASV methods was also tested by the proposed SW-ASV *via* the standard addition method. An accurate volume of the cetirizine (0.3 µg mL^{-1} in ethanol) was spiked to the tap and wastewater samples and an acceptable recovery percentage of 101±0.4 % - 107±0.6 % and 99.0±0.3%-

104.0±0.1% was achieved for the spiked cetirizine to tap and wastewater samples, respectively (Table 3). The average recovery was successfully compared with the previous data achieved by the official UV-Vis spectrophotometric method [16]. The calculated value of student *t* (*t*=1.06-1.11) and *F* (1.02- 1.79) values at 95% (n=5) for tap and wastewater samples did not exceed the tabulated ones for student *t* = 2.31 and *F* = 6.39 [47] confirming the suitability of the proposed electrochemical probe for CTZ determination.

Table 3. Analysis of cetirizine dihydrochloride in tap and wastewater (n=5) by the proposed standard addition SW-ASV and UV-Vis procedures [16]*

Sample	Added, μgmL^{-1}	SW -ASV		UV-Vis	
		Found, μgmL^{-1}	**Recovery% ,RSD**	**Found, μgmL^{-1}**	Recovery% ,RSD
Tap water	0.0	nd	-	nd	-
	10.0	10.7±0.06	107±0.6	11.0±0.05	110±0.5
	20.0	20.8±0.03	104±0.1	20.9±0.08	105±0.4
	30.0	30.3±0.11	101±0.4	30.6±0.03	102±0.1
Waste water	0.0	10.1±0.09	-	10.3±0.07	-
	10.0	20.3±0.04	103±0.4	21.0±0.09	110±0.8
	20.0	30.8±0.03	104±0.1	29.7±0.08	98.5±0.4
	30.0	39.8±0.09	99.3±0.3	40.8±0.06	103±0.2

* Mean (n=5) ± S.D.; nd.= not detected.

4. CONCLUSION & FUTURE PERSPECTIVES

The developed SW-ASV methodology for the determination of the CTZ drug on the proposed BiF/GCE provided a novel, robust, precise, and sensitive electrochemical sensor. The proposed procedure was not hindered through the interference of several imperative and regular species detected within the pharmaceutical preparations. In addition, the utilization of this BiF/GCE for CTZ revealed innumerable advantages, including: simplicity, reasonable costs, and low detection limits over the reported methods. Furthermore, the developed methodology was efficaciously employed for the analysis of CTZ in pharmaceutical preparations and tap and wastewater samples. The proposed methodology is precise, short analytical time, sensitive, economical, reproducible and offers miniaturized sample preparation for drug analysis in complex matrices. Furthermore, the present approach is favorably validated with the reported standard HPLC methods. Finally, the developed probe presents an excellent alternative to the expensive chromatographic methods for trace drug analysis in real samples.

SUPPLEMENTARY MATERIALS

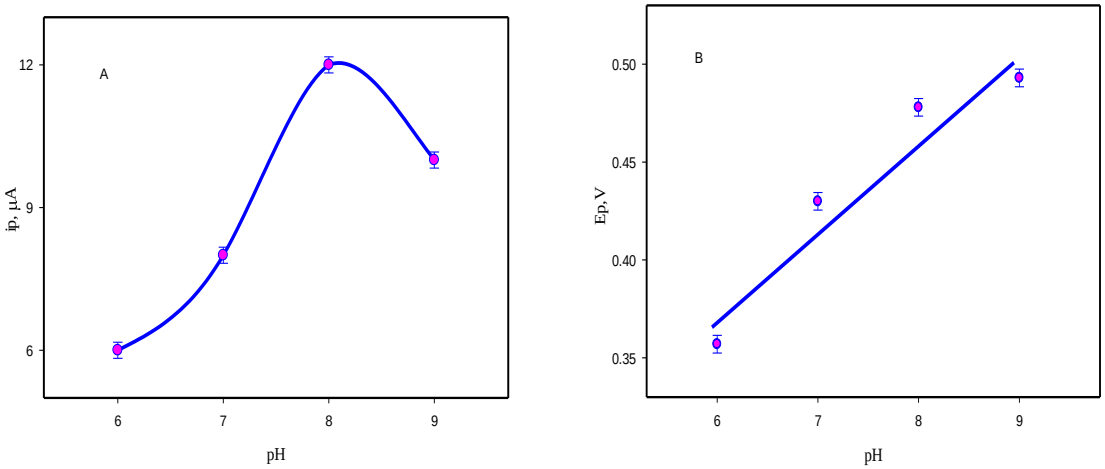

Figure S1. (A) Plot of anodic peak current $i_{p,a}$ of CTZ drug *versus* pH. **(B)** Effect of pH on anodic peak potential $E_{p,a}$ of CTZ drug at Bi/GCE *vs.* Ag/AgCl electrode.

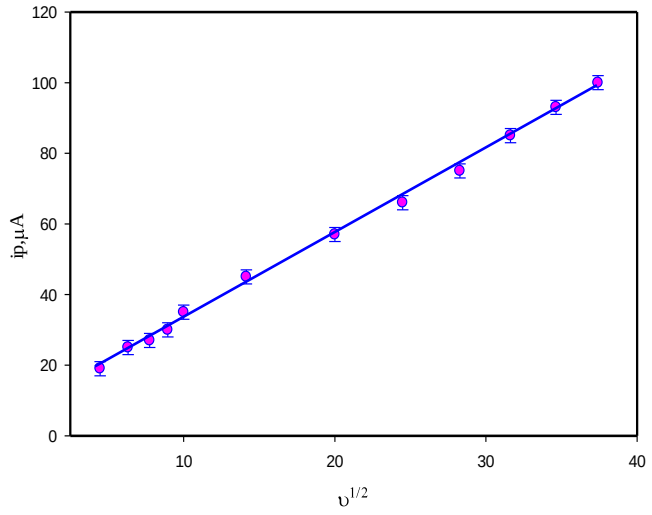

Figure S2. Plot of $i_{p,a}$ *with* square root of scan rate ($\upsilon^{1/2}$) of CTZ drug at BiF/GCE (pH 8.0).

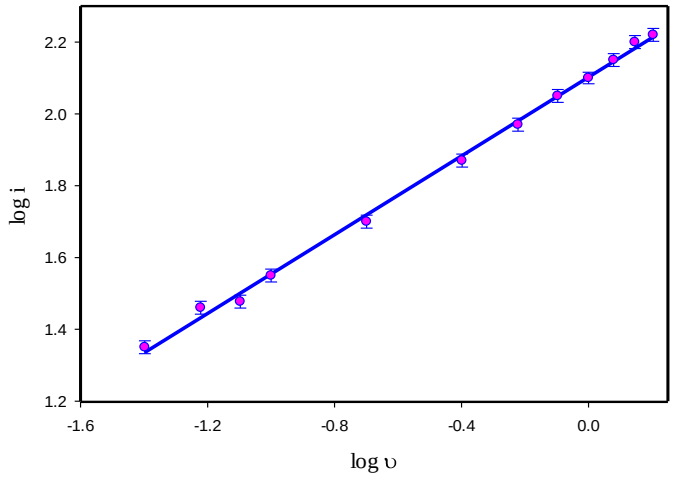

Figure S3. Influence of log anodic peak current (log $i_{p,a}$) of CTZ *versus* log ν (20 – 1400 mVs^{-1}) at BiF/GCE (pH 8.0).

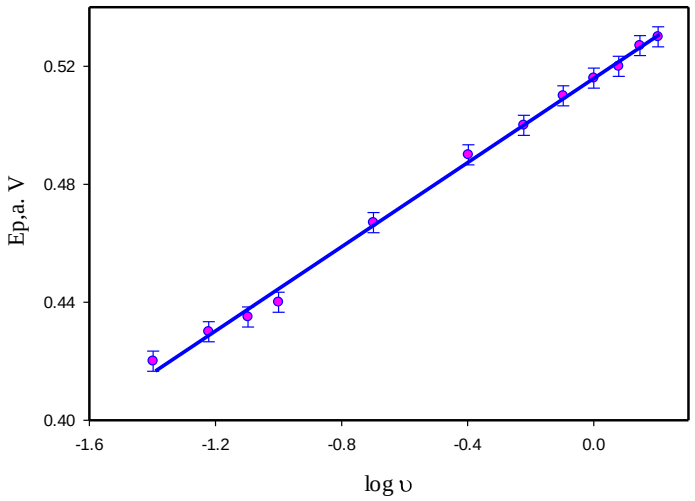

Figure S4. Effect of anodic peak potential ($E_{p,a}$) of CTZ drug *versus* log ν at BiF/GCE (pH 8.0).

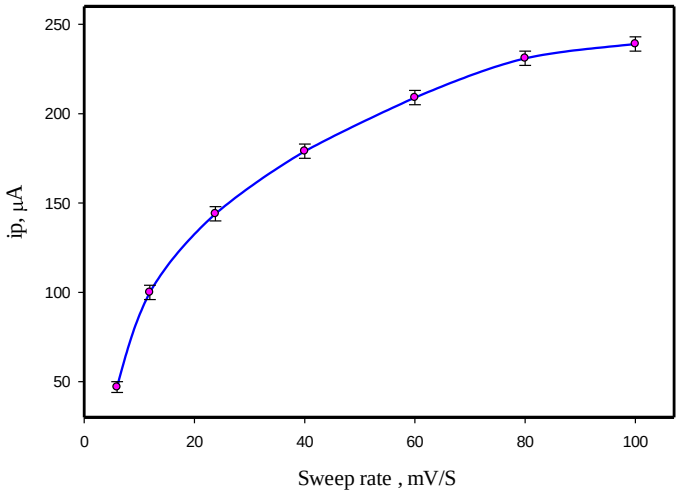

Figure S5. Influence of sweep rate on the $i_{p,a}$ of CTZ drug at BiF/GCE (pH 8.0).

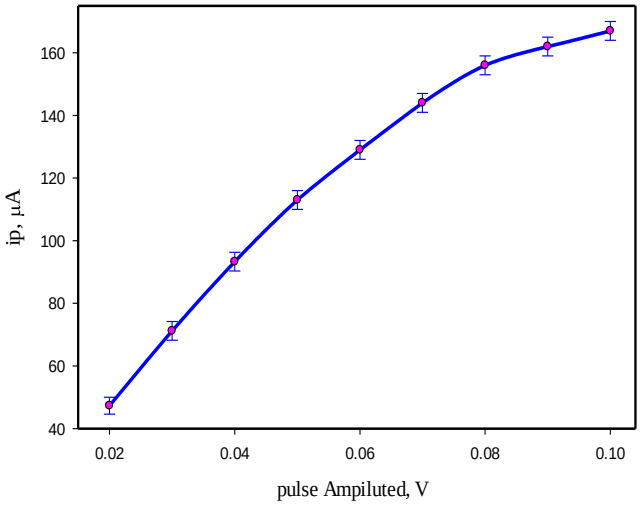

Figure S6. Effect of pulse amplitude (V) on the $i_{p,a}$ of CTZ drug at BiF/GCE (pH 8.0).

References

1. D.M. Campoli-Richards, M.M.-T. Buckley, A. Fitton, *Drugs*, 40 (1990) 762-781.
2. M.P. Curran, L.J. Scott, C.M. Perry, *Drugs*, 64 (2004) 523-561.
3. C.M. Spencer, D. Faulds, D.H. Peters, *Drugs*, 46 (1993) 1055-1080.
4. A. Pagliara, B. Testa, P.-A. Carrupt, P. Jolliet, C. Morin, D. Morin, S. Urien, J.-P. Tillement, J.-P. Rihoux, *J. Med. Chem.*, 41 (1998) 853-863.
5. S. Carson, N. Lee, S. Thakurta, Drug class review: newer antihistamines: final report update 2, (2010).
6. G. Garg, G.P. Thami, *J. Dermatol. Treat.*, 18 (2007) 23-24.
7. E. Baltes, R. Coupez, H. Giezek, G. Voss, C. Meyerhoff, M.S. Benedetti, *Fundam. Clin. Pharmacol.*, 15 (2001) 269-277.
8. J.-P. Tillement, B. Testa, F. Brée, *Biochem. Pharmacol.*, 66 (2003) 1123-1126.

9. S. Güngör, *Pharmazie,* 59 (2004) 929-933.
10. S.L. Prabhu, A. Shirwaikar, A. Shirwaikar, C.D. Kumar, G.A. Kumar, *Indian J. Pharm. Sci.*, 70 (2008) 236.
11. M.S. Raghu, K. Basavaiah, *Arab J. Basic Appl. Sci.*, 12 (2012) 33-41.
12. B. Gowda, M. Melwanki, J. Seetharamappa, *J. Pharm. Biomed. Anal.*, 25 (2001) 1021-1026.
13. S.S.R. Urs, M. Bindu, D. Ramyashree, K. Sowmya, *Asian J. Pharm. Anal.*, 10 (2020)185-188.
14. M. Moazzam, M. Asghar, M. Yaqoob, S. Ali, A. Nabi, *J. Lumin.*,36 (2020) 674-683.
15. A.F. Youssef, R.A. Farghali, *Can. J. Anal. Sci. Spectros.*, 51 (2006) 288-296.
16. A.A. Gazy, H. Mahgoub, F. El-Yazbi, M. El-Sayed, R.M. Youssef, *J. Pharm. Biomed. Anal.*, 30 (2002) 859-867.
17. N.M. Rizk, S.S. Abbas, F.A. El-Sayed, A. Abo-Bakr, *Int. J. Electrochem. Sci.*, 4 (2009) 396-406.
18. E. Baltes, R., Coupez, L. Brouwers, J. Gobert, *J. Chromatogr. B: Biomed.* Sci. Appl., 430, 74 (1988) 149-155.
19. M. Zaater, Y. Tahboub, N. Najib, *J. Pharm. Biomed. Anal.*, 22 (2000) 739-744.
20. H. Eriksen, R. Houghton, R. Green, J. Scarth, *Chromatographia*, 55 (2002) S145-S149.
21. A. Jaber, H. Al Sherife, M. Al Omari, A. Badwan, *J. Pharm. Biomed. Anal.*, 36 (2004) 341-350.
22. B. Paw, G. Misztal, H. Hopkała, J. Drozd, *pharmazie*, 57 (2002) 313-315.
23. Ü.D. Uysal, M. Tunçel, *J. Liq. Chromatogr. Relat. Technol.*, 29 (2006) 1781-1792.
24. M. Paczkowska, M. Mizera, A. Tężyk, P. Zalewski, J. Dzitko, J. Cielecka-Piontek, *Arabian J. Chem.*, 12 (2019) 4204-4211.
25. G.M. Hadad, S. Emara, W.M. Mahmoud, *Talanta*, 79 (2009) 1360-1367.
26. S. Karakuş, İ. Küçükgüzel, Ş.G. Küçükgüzel, *J. Pharm. Biomed. Anal.*, 46 (2008) 295-302.
27. S.S.a.K. Basak, *Int. J. Pharma Bio Sci.*, 9 (2018) 97-104.
28. N.P. Shetti, S.J. Malode, D.S. Nayak, K.R. Reddy, *Mater. Res. Express*, 6 (2019) 115085.
29. R.H. Patil, R.N. Hegde, S.T. Nandibewoor, *Colloids Surf., B*, 83 (2011) 133-138.
30. S. Karakaya, D.G. Dilgin, *Monatsh. Chem.*, 150 (2019) 1003-1010.
31. A.I. Vogel, Quantitative Inorganic Analysis, Longmans Group Ltd., England, 1966.
32. A. Bobrowski, A. Królicka, K. Pacan, J. Zarębski, *Electroanalysis*, 21 (2009) 2415-2419.
33. C. Prior, G.S. Walker, *Electroanalysis*, 18 (2006) 823-829.
34. J.K.B. Bernardelli, F.R. Lapolli, C.M.G.d.S. Cruz, J.B. Floriano, *J. Mater. Res.*, 14 (2011) 366-371.
35. I. Ali, V. Gupta, P. Singh, H. Pant, *Talanta*, 68 (2006) 928-931.
36. M. El-Shahawi, S. Bahaffi, T. El-Mogy, *Anal. Bioanal. Chem.*, 387 (2007) 719-725.
37. G. Zhao, H. Wang, G. Liu, Z. Wang, *Sens. Actuators, B*, 235 (2016) 67-73.
38. J. Wang, J. Lu, Ü.A. Kirgöz, S.B. Hocevar, B. Ogorevc, *Anal. Chim. Acta*, 434 (2001) 29-34.
39. T. Romih, S.B. Hočevar, A. Jemec, D. Drobne, *Electrochim. Acta*, 188 (2016) 393-397.
40. V. Jovanovski, N. Hrastnik, *Microchem. J.*, 146 (2019) 895-899.
41. A.M. Ashrafi, K. Vytřas, *Talanta*, 85 (2011) 2700-2702.
42. S. Dal Borgo, V. Jovanovski, S.B. Hocevar, *Electrochim. Acta*, 88 (2013) 713-717.
43. P.K. Kalambate, A.K. Srivastava, *Sens. Actuators, B*, 233 (2016) 237-248.
44. A.J. Bard, L.R. Faulkner, J. Leddy, C.G. Zoski, Electrochemical methods: fundamentals and applications, 2 ed., wiley New York, 2000.
45. R.S. Nicholson, I. Shain, *Anal. Chem.*, 36 (1964) 706-723.
46. M.I. Prodromidis, A.B. Florou, S.M. Tzouwara-Karayanni, M.I. Karayannis, *Electroanalysis*, 12 (2000) 1498-1501.
47. E. Laviron, L. Roullier, C. Degrand, *J. Electroanal. Chem. Interfacial Electrochem.*, 112 (1980) 11-23.
48. R. Chokkareddy, N. Bhajanthri, G. Redhi, An enzyme-induced novel biosensor for the sensitive electrochemical determination of isoniazid, *Biosensors*, 7 (2017) 21-41.
49. A. Ramadan, H. Mandil, M. Saleh, *J. Appl. Electrochem.*, 38 (2008) 1715-1720.
50. E. Fischer, C.M. van den Berg, *Anal. Chim. Acta*, 432 (2001) 11-20.

51. J.C. Miller, J.N. Miller, Statistics for Analytical Chemistry, 4 ed., Ellis-Horwood, New York, 1994.
52. A. El Walily, M. Korany, A. El Gindy, M. Bedair, *J. Pharm. Biomed. Anal.*, 17 (1998) 435-442.
53. S. Azhagvuel, R. Sekar, *J. Pharm. Biomed. Anal.*, 43 (2007) 873-878